HHS Public Access

Author manuscript

Pediatr Neurol. Author manuscript; available in PMC 2020 October 21.

Published in final edited form as:

Pediatr Neurol. 2018 July ; 84: 32–38. doi:10.1016/j.pediatrneurol.2018.04.004.

Quantitative Apparent Diffusion Coefficient Mapping May Predict Seizure Onset in Children With Sturge-Weber Syndrome

Anna L. R. Pinto[a,1,*], **Yangming Ou**[b,1], **Mustafa Sahin**[a], **P. Ellen Grant**[b]

[a]Department of Neurology, Boston Children's Hospital, Boston, Massachusetts

[b]Departments of Medicine and Radiology, Boston Children's Hospital, Boston, Massachusetts

Abstract

Background: Sturge-Weber syndrome (SWS) is often accompanied by seizures, stroke-like episodes, hemiparesis, and visual field deficits. This study aimed to identify early pathophysiologic changes that exist before the development of clinical symptoms and to evaluate if the apparent diffusion coefficient (ADC) map is a candidate early biomarker of seizure risk in patients with SWS.

Methods: This is a prospective cross-sectional study using quantitative ADC analysis to predict onset of epilepsy. Inclusion criteria were presence of the port wine birthmark, brain MRI with abnormal leptomeningeal capillary malformation (LCM) and enlarged deep medullary veins, and absence of seizures or other neurological symptoms. We used our recently developed normative, age-specific ADC atlases to quantitatively identify ADC abnormalities, and correlated presymptomatic ADC abnormalities with risks for seizures.

Results: We identified eight patients (three girls) with SWS, age range of 40 days to nine months. One patient had predominantly LCM, deep venous anomaly, and normal ADC values. This patient did not develop seizures. The remaining seven patients had large regions of abnormal ADC values, and all developed seizures; one of seven patients had late onset seizures.

Conclusions: Larger regions of decreased ADC values in the affected hemisphere, quantitatively identified by comparison with age-matched normative ADC atlases, are common in young children with SWS and were associated with later onset of seizures in this small study. Our findings suggest that quantitative ADC maps may identify patients at high risk of seizures in SWS, but larger prospective studies are needed to determine sensitivity and specificity.

Keywords

Sturge-Weber syndrome; Seizure; ADC map; Neuroimaging

Introduction

Sturge-Weber syndrome (SWS) is a segmental neurovascular disease associated with a capillary malformation caused by a somatic mutation in the affected tissue. These lesions are

*Corresponding author. Anna.Pinto@childrens.harvard.edu (A.L.R. Pinto).

[1]These authors contributed equally to this study.

caused by activating mutations in the gene *GNAQ*, encoding the $G\alpha_q$ subunit.[1] The diagnosis is often made during the neonatal period because of the presence of a port wine birthmark.[2] The extension and the location of the birthmark have been associated with increased risk of brain involvement. The vascular malformation of the brain consists of hypoplastic cortical vessels associated with enlarged and tortuous leptomeningeal vessels, as well as deep venous anomalies. One of the primary mechanisms of brain insult in SWS is thought to be poor regional cerebral perfusion due to impaired venous drainage of the affected regions. The most common neurological manifestations of SWS are seizures, stroke-like episodes, hemiparesis, and visual field deficits.[2]

Early presymptomatic diagnosis could lead to (1) a more accurate estimation of prognosis, (2) better understanding of neurological symptoms, and (3) a more accurate and timely prediction of response to therapy in this population.[3] In particular, if we can identify early predictors of seizure onset, it may be possible to therapeutically intervene and prevent the devastating regional parenchymal atrophy that is typical in this disorder.

Nevertheless, early presymptomatic diagnosis remains a challenge. T1-weighted magnetic resonance imaging (MRI) with gadolinium contrast is the current standard neuroimaging sequence for SWS diagnosis. However, contrast injection is invasive, repeated gadolinium injections can lead to gadolinium deposition, and postcontrast sequences have low sensitivity for the early diagnosis of SWS.[3,4] New MRI sequences have drawn increasing attention for the early diagnosis of SWS. In particular, apparent diffusion coefficient (ADC) maps (derived from diffusion tensor MRI) are of special consideration.[5] ADC maps quantify the regional magnitude of water diffusion.[6] Abnormally low ADC values indicating decreased diffusion have been proven to be informative for SWS diagnosis and prognosis.[2,5] However, a fundamental issue hindering further exploration of ADC values as biomarkers in SWS is the lack of a quantitative, standardized, and objective way to determine whether ADC values are abnormal. Because of this, studies report 20% to 40% intra- or interexpert variability when interpreting abnormalities in pediatric ADC maps.[7,8] For example, Fig 1 shows the ADC maps of four patients. Visually determining if there are regions of decreased ADC is subjective and therefore prone to variability.

To address the uncertainties in interpreting neonatal or pediatric ADC maps, we recently developed the first series of age-specific, normative ADC atlases.[9] Our atlases quantified the normal range of ADC variations in space (at various brain locations) and in time (at various ages in the first six years of life). This approach allowed development of computer-aided detection algorithms to quantitatively and objectively detect abnormal ADC values (and hence subtle diffusion abnormalities).[10,11] Our preliminary results showed that atlas-based ADC abnormality detection can reach an accuracy comparable with the consensus of human experts in identifying regions of neonatal hypoxic-ischemic brain injury.[12]

The main objective of this pilot study was to investigate whether our age-matched normative ADC atlases can allow detection of early, subtle, and presymptomatic abnormalities in patients with SWS, and whether the ADC abnormalities identified can serve as a radiological biomarker for later seizure onset in patients with SWS. Thus we hypothesize

that atlas-identified regions of abnormally low ADC values in affected areas can predict seizure onset in patients with SWS.

Methods

Institutional review board approval and consent

This is a prospective study. Clinical and neuroimaging data were collected from children with SWS in this observational cross-sectional study at Boston Children's Hospital. The study period was from February 2010 to February 2017. The study was approved by the institutional review board at Boston Children's Hospital, and written informed consent of the parent or legal guardian was obtained.

Inclusion criteria

We included patients with SWS based on the presence of a port wine birthmark (PWB) involving the forehead and the upper eyelid. Brain involvement was identified when leptomeningeal venous malformation or enlarged deep medullary veins (with or without enlarged choroid plexus) on contrast-enhanced MRI were present. We excluded patients with a diagnosis of other cutaneous vascular malformations, such as Klipple-Trenaunay syndrome, PHACE (posterior fossa malformations, facial hemangiomas, arterial anomalies, cardiac anomalies and aortic coarctation, eye anomalies) syndrome, and diffuse neonatal hemangiomatosis.

Imaging protocol

Diffusion tensor MRI was performed on a Siemens Trio 3T scanner with a 32-channel head coil. The diffusion protocol was repetition time = 7500 to 9500 ms, echo time = 80 to 115 ms, matrix = 128 × 128 × 60, voxel size = 2 × 2 × 2 mm, b value = 1000 s/mm^2 with the number of diffusion encoding directions = 32 and five b = 0 acquisitions. ADC maps were automatically generated by the software embedded in the scanner and took about five minutes per patient. Patients were not sedated during the MRI scan.

Atlas-quantified normal variation

Figure 2 visualizes the middle-brain axial slices of our age-specific normative ADC atlases. Ou et al.[9] has more detail on atlas construction. We sampled the first year of life in greater detail to capture the rapid changes during this period. Overall, there are 10 age groups as shown in Fig 2: the first two weeks of life, the remainder of the first quarter of life; the other three quarters in the first year of life; and ages 1 to 2, 2 to 3, 3 to 4, 4 to 5, and 5 to 6 years. The first row shows the mean ADC values throughout the brain (denoted as μ), whereas the second row shows the S.D. ADC values (denoted as σ). Figure 3 uses the first two weeks of life (i.e., the atlas in our first age group) as an example: voxel-wise calculation of the mean (μ) ± 1 or 2 S.D. (σ) ADC maps gauges the normal range of ADC variation in this age group. Gauging the spatiotemporal normal ADC variations serves as the basis for our atlas-based ADC mapping and abnormality detection.

Atlas-based abnormality identification

A patient's ADC map first went through automated skull stripping[13] to remove nonbrain tissue or structures. To enable voxel-by-voxel comparison between the patient's ADC map and the age-matched atlases, the age-matched atlas (the mean atlas map) was spatially transformed into the skull-stripped patient ADC map. This method was done by using the DRAMMS deformable registration tool,[14] which has been extensively validated in image registration tasks, including registration between normal atlases and abnormality-bearing images.[15] The same deformation was used to also spatially transform the S.D. ADC map of the same age group into the patient space. Then, the patient's ADC map was converted into a Z map, consisting of Z values at every voxel in the patient space. The Z value at a voxel quantifies the number of S.D. patient ADC value deviated from the average ADC value of the same anatomic location in the atlas, that is, the subtraction of the patient's ADC value from the mean ADC value at the corresponding location in the atlas divided by the S.D. ADC value at the corresponding location in the atlas.[10] Those brain voxels having $Z < -2$ (i.e., at least 2 S.D. below the population mean ADC) were considered abnormal regions of decreased diffusion.

Results

Eight patients (three girls) whose first brain MRI was obtained before clinical symptoms were enrolled in our study. Figure 4 shows the detected abnormalities using the proposed techniques before the onset of seizure.

All patients were identified at birth by the PWB involving the forehead and the upper eyelids, indicating a higher risk of brain involvement. The first brain MRI was obtained during the first year of life, and the mean age for first imaging was 4.4 months (max = 9 months and min = 1.5 months). Seven patients developed seizures, and one remains asymptomatic. In subjects who developed symptoms, the interval between the acquisition of the presymptomatic brain MRI and first clinical seizure was approximately 4.7 months (in four patients, the interval was within three months, and the longest interval was 20 months) (Table 1). The patients were followed up for a minimum of two years.

Patient 1 is now a four-year old boy with normal neurological examination and no clinical symptoms. His brain MRI has shown progressive enlargement of the deep venous system and leptomeningeal enhancement involving two lobes (occipital and parietal); however, no volume loss, no calcifications, and no white matter signal abnormalities were noted. No signs of regional diffusion decreases were found in our atlas-based abnormality detection (Fig 4).

The brain MRI result of Patient 2 showed leptomeningeal enhancement involving the occipital and parietal regions bilaterally. There were no signs of brain atrophy, calcifications, obvious enlargement of the deep venous system, and no white matter signal abnormalities. However, atlas-based analysis found subtle regional ADC decreases in the left occipital lobe and the left thalamus (Fig 4). He has been followed up closely and his first seizure occurred at age 24 months. He has had two breakthrough seizures but has been stable on combination of oxcarbazepine and levetiracetam.

Patient 3 presented with focal motor seizure one month after the first brain MRI. She has been stable on monotherapy with levetiracetam. At age 19 months, she had one brief stroke-like event after mild head trauma. The presymptomatic brain MRI showed early signs of abnormal T1 and T2 signals involving the right occipital and parietal lobes. ADC decreases were also most marked in the right occipital region (Fig 4).

Patient 4 first presented with prolonged focal motor seizures requiring intensive care unit admission. She continued with breakthrough seizures despite therapeutic doses of levetiracetam, oxcarbazepine, and clobazam. This patient has been evaluated for possible epilepsy surgical intervention. Presymptomatic brain MRI showed extensive leptomeningeal capillary malformation (LCM) and T1 and T2 abnormal signals in the left occipital, parietal, temporal, and frontal regions. ADC decreases were found throughout the left hemisphere, most marked in the temporal-occipital and frontal regions (Fig 4). The follow-up brain MRI showed progressive changes with cortical atrophy and calcifications.

Patient 5 exhibited left hemianopsia documented during clinic visit at age 5 months, and his first seizure occurred at age 4 months. His first stroke-like event occurred at 22 months old. He has been stable on combination of levetiracetam and oxcarbazepine. His first brain MRI at 40 days of life showed extensive right hemispheric abnormalities with decreased ADC values in the right occipital region greater than the right temporal region (Fig 4). Follow-up brain MRI showed bilateral asymmetric changes (right > left) characterized by cortical atrophy, LCM, deep venous anomaly, and calcification.

Patients 6 developed seizures at six months old. The seizures were focal motor and apneic seizures and were highly refractory to the combination of antiseizure medications. At age 10 months, he underwent hemispherectomy and has been seizure free. The presymptomatic brain MRI at three months old showed extensive left hemispheric abnormalities with deep venous anomaly, LCM, T1 (parenchymal atrophy), and T2 abnormal signals. Diffuse bilateral ADC decreases were found (Fig 4).

Patient 7 presented with prolonged focal motor seizures and Todd paralysis. He also had stroke-like events in the settings of febrile illness. The seizures are intractable despite therapeutic doses of multiple medications, and the patient has been evaluated for epilepsy surgery. The brain MRI showed right frontal atrophy, T2 abnormal signal, and increased medullary veins. There is also evidence of calcification in the right frontal region. The typical SWS findings are seen over the right hemisphere only. Diffuse bilateral ADC decreases were found (Fig 4). The increased values in the Z map of Patient 7 may be due to delayed myelination.

Patient 8 developed seizures at two months. The seizures were described as left arm clonic rhythmical movements; the seizure pattern progressed quickly with secondary generalized convulsion and apneic seizures. Given the intractability of the seizures with multiple anti-epileptic drugs, the patient underwent hemispherectomy at age 6 months. The patient remained seizure free and all antiseizure medications were discontinued. The first baseline brain MRI showed extensive LCM, T1 (brain parenchymal atrophy), and marked T2

abnormal signals in the right hemisphere. Diffuse right hemispheric decreased ADC values were also noted (Fig 4).

The neurological outcomes are shown in Table 2 using the SWS neurological rating system published by Reidy et al. in 2014.[16]

Overall, all seven patients who developed seizures at a later stage had regions of abnormally decreased ADC values automatically identified on their presymptomatic MRI when using age-matched atlases for comparison. The only patient (Patient 1) for whom the age-matched normative ADC atlas analysis did not detect diffusion abnormality has not developed seizures with follow-up at age 4 years.

Furthermore, as Fig 5 shows in two representative patients, our proposed ADC mapping has found abnormalities that were not pronounced in T1-weighted images, regardless of using post contrast or not. The findings are similar in other patients in our cohort, which highlight the potential of the proposed ADC mapping to capture abnormalities also detected by gadolinium contrast enhancement images in this cohort.

Discussion

SWS can be suspected at birth because of evidence of PWB in high-risk distribution. Early presymptomatic imaging is often obtained to screen for associated brain abnormalities. There is no consensus regarding the optimal timing to acquire the imaging. There is also no consensus about which brain MRI sequences can accurately identify presymptomatic brain abnormalities,[17,18] although T1-weighted MRI with gadolinium enhancement (T1 + Gad) is usually used. Compared with the T1 + Gad sequence, where the use of a contrast agent may be linked with long-term neurotoxicity,[19,20] the ADC map derived from the diffusion MRI sequence is contrast-free. This study conducted one of the first studies using age-matched ADC atlases to recognize regions of decreased diffusion in seven presymptomatic patients, who later developed seizures, and no diffusion abnormalities in one patient, who remained asymptomatic. ADC maps provide valuable information about early changes in the white matter affecting the water diffusion secondary to the evolution of SWS. Our recently developed age-specific normative ADC atlases offer opportunities to objectively capture ADC abnormalities, which are otherwise subject to uncertainties.[21]

T1 postgadolinium sequences[3] are typically used for SWS, but noncontrast MRI sequences are needed,[22] given the recent warning from the Food and Drug Administration and studies regarding the repeated use of contrast agents for brain MRI studies.[22] The classic brain MRI finding in SWS by T1 postgadolinium sequence is leptomeningeal enhancement, which may extend over the entire hemisphere and, when unilateral, is typically ipsilateral to the PWB. In addition, if no invasive injection is required, SWS infants may be able to be monitored with MRI scans obtained without sedation or anesthesia. This method is also attractive, given the Food and Drug Administration warnings against the repeated use of the agents used for MRI.[23] Thus ADC maps, which are quantitative parameter maps derived from diffusion MRI and are contrast agent-free, should be further evaluated and validated as an alternative and potentially unbiased effective means for SWS diagnosis and prognosis.

Figure 4 shows that our ADC mapping successfully captured presymptomatic abnormalities in all seven patients with SWS who later on developed seizures. Figure 5 further shows more pronounced abnormalities as found in the proposed ADC mapping than in the gadolinium contrast enhancement images, suggesting the need to further explore the potential of our ADC mapping in future larger scale studies.

The pathologic correlates of decreased ADC values in the white matter are unclear. Recent work has determined that the p.R183Q *GNAQ* mutation is primarily present in the endothelial cells within SWS and capillary malformation lesions, suggesting a cell-autonomous effect, although the effects of the mutation on endothelial cell biology are not currently understood.[24] Calcification, neuronal loss, and gliosis are likely secondary to brain injury resulting from venous stasis and impaired brain perfusion rather than being primarily the result of the somatic mutation.[25] ADC decreases are also unlikely to be a primary result of the somatic mutation. We postulate that ADC decreases may be due to early myelination in reaction to prolonged subclinical seizures or ischemic insult. In SWS, the observed damage of brain tissue underlying the LMC is thought to be secondary, caused by impaired venous blood flow resulting in chronic ischemia, neuronal loss, atrophy, and calcification, thus leading to cortical and white matter abnormalities on imaging. However, the correlation of *GNAQ* mutations and magnetic resonance abnormalities, and the exact course of ADC decrease will need larger scale prospective studies to explore.

In our group of patients, six of eight patients had other abnormal features in the presymptomatic brain MRI characterized by white matter decreased T2 signal, T1 abnormality suggestive of cortical atrophy. One subject had regional ADC decreases when only mild leptomeningeal enhancement was present, but no other abnormal MRI findings were noted. Subject 1, with no signs of seizure after four years, had an MRI with mild leptomeningeal enhancement and associated deep venous anomaly. Therefore there is no one-to-one correspondence between ADC changes and findings on other MRI sequences.

One major limitation of our study is the small sample size, with the inclusion of only one asymptomatic patient. Another limitation is the potential variability of ADC values across sites and scanners, which can be up to, 5% to 10%.[26–28] Therefore to better facilitate future trials, we will need to show that our atlases apply to multisite or scanner data. Our ongoing work also includes designing a more robust algorithm that can identify more subtle abnormalities in multisite image data. However, even with these limitations, our study showed promising results for ADC maps to serve as a means to identify patients with high risk of seizures.

Our future work will also extend beyond presymptomatic abnormality detection into seizure prediction. Approximately 75% and up to 90% of patients with SWS will develop epilepsy.[29] Early onset of seizures and medically resistant epilepsy are indicative of a poor prognosis.[3] Advanced neuroimaging studies have brought a greater understanding of the pathogenesis and the clinical and imaging manifestations of SWS. Our future work will require a much larger cohort to further test the sensitivity and the specificity of quantitative ADC analysis in predicting the onset of seizures. This noninvasive and contrast agent-free early biomarker, if

carefully validated, can lead to development of a novel neuroprotective strategy and means to monitor the progression of the disease.

Another piece of future work is to extend beyond the current cross-sectional study into a longitudinal study of the natural history of the disease progression. Correlating ADC deviations with findings in other imaging sequences routinely acquired clinically[30,31] can be helpful in understanding the natural course and outcome of this developmental disease. This approach will determine if the use of multiple sequences provides higher prognostic value than any one sequence alone. In addition, such longitudinal information is needed to optimize timing and the number of brain MRIs, as well as to determine if contrast agents are required to diagnose brain involvement and to better predict neurological outcomes in the SWS population.

Conclusions

Detection of subtle diffusion abnormalities, traditionally a subjective interpretation and a challenge to expert radiologists, can be standardized and objective when age-specific normative ADC atlases are used for comparison. Our pilot study suggests that the presymptomatic presence of regional ADC abnormalities is correlated with the development of seizures. However, further validation in larger scale and multisite studies is required.

Acknowledgements

The authors are indebted to the generosity of the SWS families and patients who contributed their time and effort to this study. This project was supported by a grant from the Translational Neuroscience Center and Credit Unions Kids at Heart.

References

1. Shirley MD, Tang H, Gallione CJ, et al. Sturge-Weber syndrome and port-wine stains caused by somatic mutation in GNAQ. N Engl J Med. 2013;368:1971–1979. [PubMed: 23656586]
2. Comi AM. Update on Sturge-Weber syndrome: diagnosis, treatment, quantitative measures, and controversies. Lymphat Res Biol. 2007;5:257–264. [PubMed: 18370916]
3. Comi AM. Presentation, diagnosis, pathophysiology, and treatment of the neurological features of Sturge-Weber syndrome. Neurologist. 2011;17:179–184. [PubMed: 21712663]
4. Pinto AL, Chen L, Friedman R, et al. Sturge-Weber syndrome: brain magnetic resonance imaging and neuropathology findings. Pediatr Neurol. 2016;58:25–30. [PubMed: 26706049]
5. Lo W, Marchuk DA, Ball KL, et al. Updates and future horizons on the understanding, diagnosis, and treatment of Sturge-Weber syndrome brain involvement. Dev Med Child Neurol. 2012;54:214–223. [PubMed: 22191476]
6. Sener RN. Diffusion MRI: apparent diffusion coefficient (ADC) values in the normal brain and a classification of brain disorders based on ADC values. Comput Med Imaging Graph. 2001;25:299–326. [PubMed: 11356324]
7. Goergen SK, Ang H, Wong F, et al. Early MRI in term infants with perinatal hypoxic-ischaemic brain injury: interobserver agreement and MRI predictors of outcome at 2 years. Clin Radiol. 2014;69:72–81. [PubMed: 24210250]
8. Cheong JL, Coleman L, Hunt RW, et al. Prognostic utility of magnetic resonance imaging in neonatal hypoxic-ischemic encephalopathy: substudy of a randomized trial. Arch Pediatr Adolesc Med. 2012;166:634–640. [PubMed: 22751877]

9. Ou Y, Zollei L, Retzepi K, et al. Using clinically acquired MRI to construct age-specific ADC atlases: quantifying spatiotemporal ADC changes from birth to 6-year old. Hum Brain Mapp. 2017;38:3052–3068. [PubMed: 28371107]
10. Ou Y, Jaims C, Gollub RL, et al. Neonatal Brain Injury Detection in MRI: An Atlas-based Fully-Automatic Approach. Paper presented at: Human Brain Mapping Annual Meeting; June 18, 2015.
11. Jaims C, Ou Y, Shih J, et al. Apparent Diffusion Coefficient Z-score Maps Compared to Normative Atlas in Hypoxic Ischemic Encephalopathy. Paper presented at: ASNR 53rd Annual Meeting & The Foundation of the ASNR Symposium 2015; April 25, 2015.
12. Ou Y, Gollub RL, Wang J, et al. MRI Detection of Neonatal Hypoxic Ischemic Encephalopathy: Machine v.s. Radiologists. Paper presented at: Organization for Human Brain Mapping (OHBM); June 25, 2017.
13. Ou Y, Gollub RL, Retzepi K, et al. Brain extraction in pediatric ADC maps, toward characterizing neuro-development in multi-platform and multi-institution clinical images. Neuroimage. 2015;122:246–261. [PubMed: 26260429]
14. Ou Y, Sotiras A, Paragios N, Davatzikos C. DRAMMS: deformable registration via attribute matching and mutual-saliency weighting. Med Image Anal. 2011;15: 622–639. [PubMed: 20688559]
15. Ou Y, Akbari H, Bilello M, Da X, Davatzikos C. Comparative evaluation of registration algorithms in different brain databases with varying difficulty: results and insights. IEEE Trans Med Imaging. 2014;33:2039–2065. [PubMed: 24951685]
16. Reidy TG, Suskauer SJ, Bachur CD, McCulloch CE, Comi AM. Preliminary reliability and validity of a battery for assessing functional skills in children with Sturge-Weber syndrome. Childs Nerv Syst. 2014;30:2027–2036. [PubMed: 25344741]
17. Dutkiewicz AS, Ezzedine K, Mazereeuw-Hautier J, et al. A prospective study of risk for Sturge-Weber syndrome in children with upper facial port-wine stain. J Am Acad Dermatol. 2015;72:473–480. [PubMed: 25592619]
18. Piram M, Lorette G, Sirinelli D, Herbreteau D, Giraudeau B, Maruani A. Sturge-Weber syndrome in patients with facial port-wine stain. Pediatr Dermatol. 2012; 29:32–37. [PubMed: 21906147]
19. Blumfield E, Moore MM, Drake MK, et al. Survey of gadolinium-based contrast agent utilization among the members of the Society for Pediatric Radiology: a Quality and Safety Committee report. Pediatr Radiol. 2017;47:665–673. [PubMed: 28283728]
20. Olchowy C, Cebulski K, Lasecki M, et al. The presence of the gadolinium-based contrast agent depositions in the brain and symptoms of gadolinium neurotoxicity—a systematic review. PLoS ONE. 2017;12:e0171704.
21. Beaulieu A A space for measuring mind and brain: interdisciplinarity and digital tools in the development of brain mapping and functional imaging, 1980–1990. Brain Cogn. 2002;49:13–33. [PubMed: 12027389]
22. Malayeri AA, Brooks KM, Bryant LH, et al. National institutes of health perspective on reports of gadolinium deposition in the brain. J Am Coll Radiol. 2016; 13:237–241. [PubMed: 26810815]
23. FDA. FDA evaluating the risk of brain deposits with repeated use of gadolinium-based contrast agents for magnetic resonance imaging (MRI) safety announcement 2015.
24. Huang L, Couto JA, Pinto A, et al. Somatic GNAQ mutation is enriched in brain endothelial cells in Sturge-Weber syndrome. Pediatr Neurol. 2017;67:59–63. [PubMed: 27919468]
25. Wetzel-Strong SE, Detter MR, Marchuk DA. The pathobiology of vascular malformations: insights from human and model organism genetics. J Pathol. 2017; 241:281–293. [PubMed: 27859310]
26. Walker L, Chang LC, Nayak A, et al. The diffusion tensor imaging (DTI) component of the NIH MRI study of normal brain development (PedsDTI). Neuroimage. 2016;124(pt B):1125–1130. [PubMed: 26048622]
27. Huo J, Alger J, Kim H, et al. Between-scanner and between-visit variation in normal white matter apparent diffusion coefficient values in the setting of a multicenter clinical trial. Clin Neuroradiol. 2016;26:423–430. [PubMed: 25791203]
28. Giannelli M, Sghedoni R, Iacconi C, et al. MR scanner systems should be adequately characterized in diffusion-MRI of the breast. PLoS ONE. 2014;9: e86280.

29. Pinto A, Sahin M, Pearl PL. Epileptogenesis in neurocutaneous disorders with focus in Sturge Weber syndrome. F1000Res. 2016;5.

30. Adams ME, Aylett SE, Squier W, Chong W. A spectrum of unusual neuroimaging findings in patients with suspected Sturge-Weber syndrome. AJNR Am J Neuroradiol. 2009;30:276–281. [PubMed: 19050205]

31. Wu J, Tarabishy B, Hu J, et al. Cortical calcification in Sturge-Weber syndrome on MRI-SWI: relation to brain perfusion status and seizure severity. J Magn Reson Imaging. 2011;34:791–798. [PubMed: 21769978]

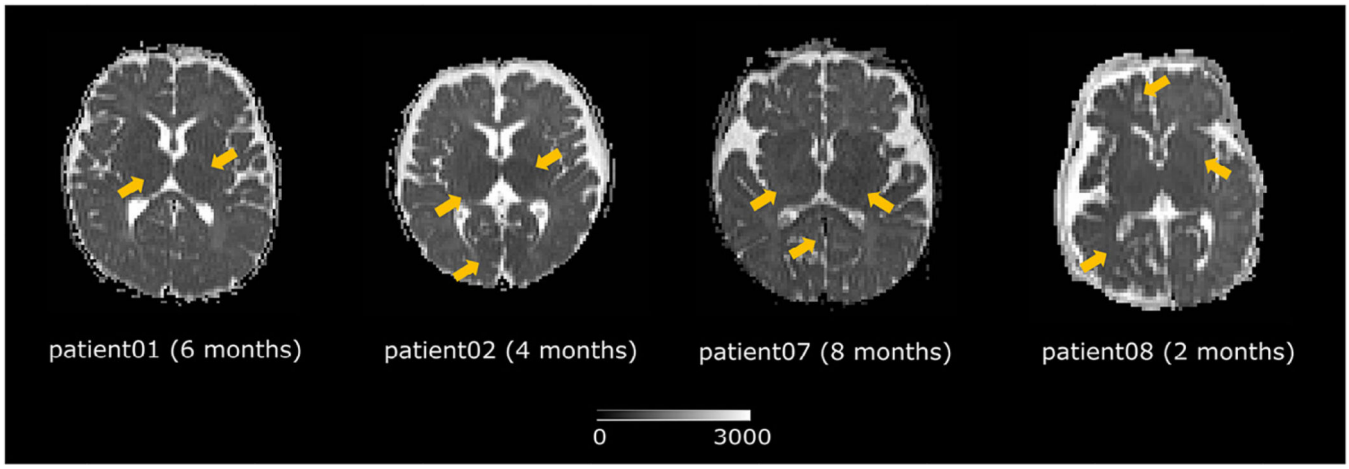

FIGURE 1.

Do the regions indicated by yellow arrows exhibit abnormally low ADC values? ADC maps have great potentials for early diagnosis and prognosis of Sturge-Weber syndrome. This figure highlights the need for an objective, standardized, and quantitative way to identify regional ADC abnormalities. ADC, apparent diffusion coefficient.

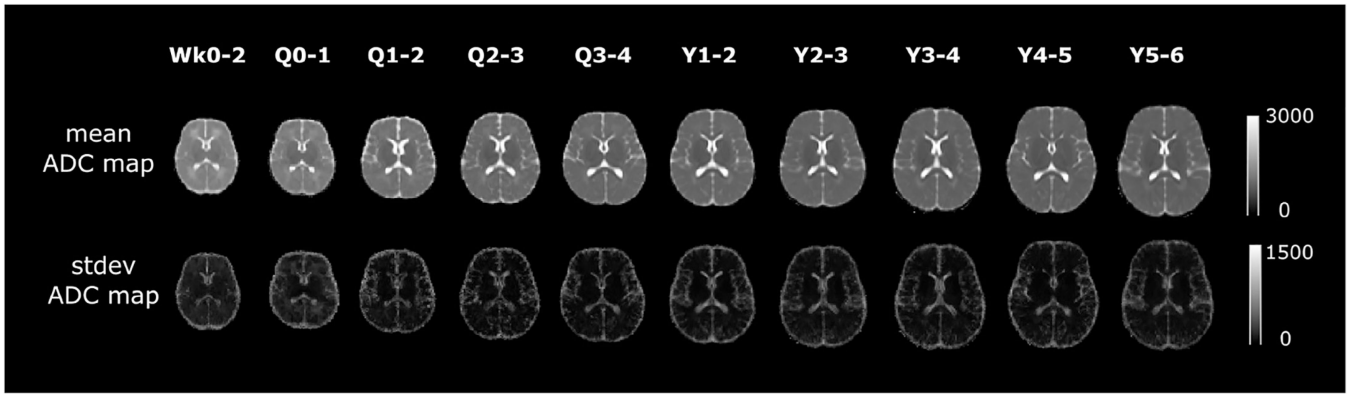

FIGURE 2.

Our age-specific normative ADC atlases in the first six years of life. The unit of ADC values is squared micrometer per second. ADC, apparent diffusion coefficient; Q, quarter; Wk, week; Y, year.

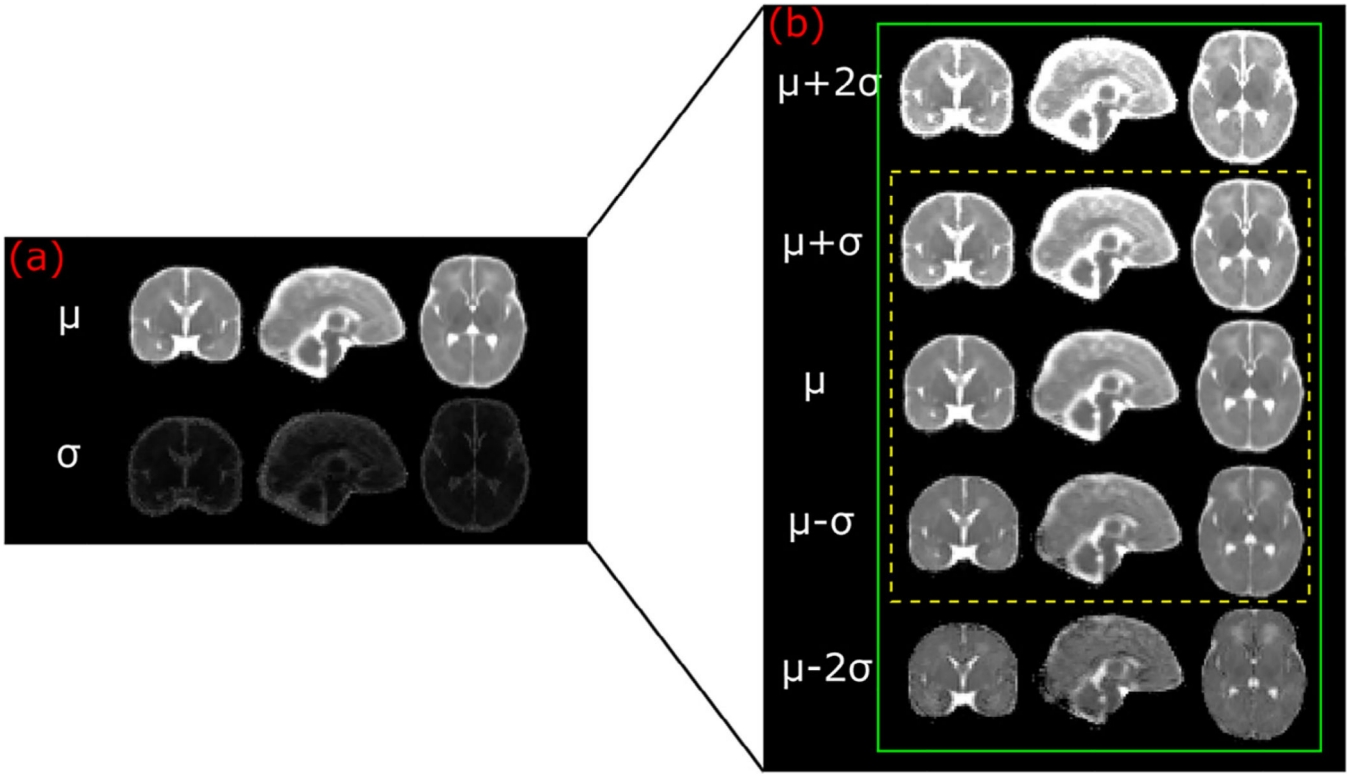

FIGURE 3.
Atlas-quantified normal range of apparent diffusion coefficient variations for the Wk0–2 age group.

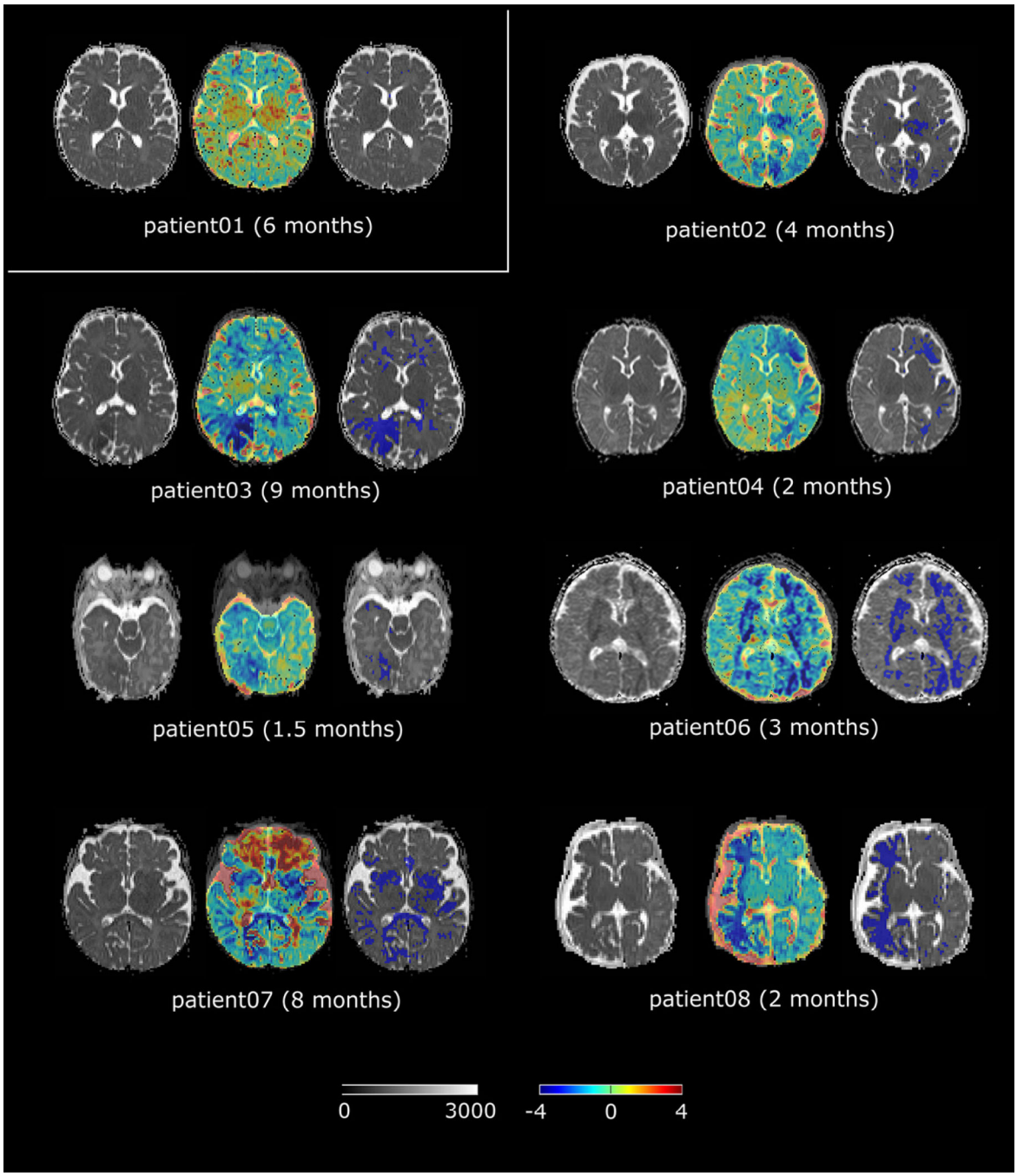

FIGURE 4.

Atlas detected ADC abnormalities. This figure answers the question in Fig 1. Abnormal regions were detected in all seven patients who went on to develop seizures. For every patient, the left panel shows the original patient ADC map; the middle panel shows the computed Z map overlaid on the patient's ADC map at the 50% transparency (a color scale is shown at the bottom of Fig 4); and the right panel shows the regions having abnormally low ADC values (where Z <−2) in blue as overlaid on the patient's ADC map. ADC, apparent diffusion coefficient.

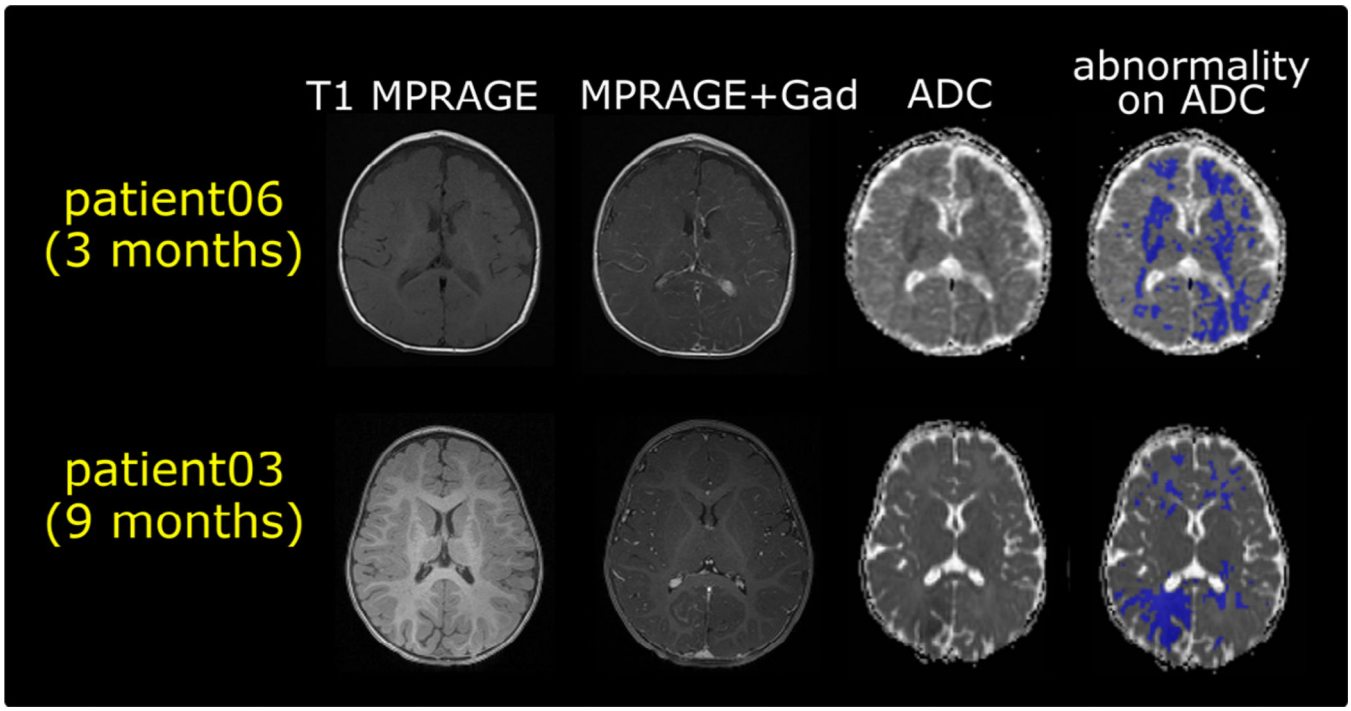

FIGURE 5.

Two representative patients' multimodal magnetic resonance images (T1 with and without Gad contrast enhancements, ADC map, and the proposed ADC mapping).ADC, apparent diffusion coefficient; Gad, gadolinium; MPRAGE, magnetization-prepared rapid gradient-echo.

TABLE 1.

Demographics and Clinical Symptoms

Patient ID	Gender	Age at First Brain MRI	Age at First Clinical Symptom	Neurological Symptom
1	M	6 months	NA	NA
2	M	4 months	2 years	Seizure
3	F	9 months	10 months	Seizure or stroke-like events
4	F	2 months	3 months	Seizures
5	M	1.5 months	4 months	Seizure or stroke-like events
6	M	3 months	6 months	Seizures
7	M	8 months	8 months	Seizures or stroke-like events
8	F	2 months	2 months	Seizure

Abbreviations:

F = Female

M = Male

MRI = Magnetic resonance imaging

NA = Not applicable

TABLE 2.

SWS Neurological Rating System (Reidy et al.[16])

Patient ID	Age Score (y)	Seizure Score*	Hemiparesis Score†	Visual Field Cut Score‡	Cognitive Function Score§
1	4	0	0	0	0
2	3	1	0	0	2
3	2	1	1	1	1
4	2	3	2	2	2
5	3	2	2	2	3
6	3	1	4	2	3
7	4	3	2	0	4
8	4	1	3	2	3

*Seizure score (0, none ever; 1, one or more seizures, currently controlled; 2, breakthrough seizures; 3, monthly seizures; 4, at least weekly seizures).

†Hemiparesis score (0, no weakness or posturing; 1, mild posturing intermittently; 2, fine motor impairments only; 3, significant fine and gross motor impairments; 4, severe fine and gross motor impairment).

‡Visual field-cut score (0, no field cut; 1, partial homonymous hemianopsia; 2, full homonymous hemianopsia visual field cut).

§Cognitive function score—infant or preschool (0, normal; 1, mild speech delay but comprehends well; 2, mild delay in speech and comprehension; 3, moderately delayed speech; 4, severely delayed speech; 5, profoundly delayed speech with little or no comprehension).